Toward a Virtual Neuromuscular Control for Robust Walking in Bipedal Robots

Zachary Batts, Seungmoon Song, and Hartmut Geyer

***Abstract*— Walking controllers for bipedal robots have not yet reached human levels of robustness in locomotion. Imitating the human motor control might be an alternative strategy for generating robust locomotion in robots. We seek to control bipedal robots with a specific neuromuscular human walking model proposed previously. Here, we present a virtual neuromuscular controller, VNMC, that emulates this neuromuscular model to generate desired motor torques for a bipedal robot. We test the VNMC on a high-fidelity simulation of the ATRIAS bipedal robot constrained to the sagittal plane. We optimize the control parameters to tolerate maximum ground-height changes, which resulted in ATRIAS walking on a terrain with up to $\pm$7 cm height changes. We further evaluate the robustness of the optimized controller to external and internal disturbances. The optimized VNMC adapts to 90% of random terrains with ground-height changes up to $\pm$2 cm. It endures 95% of $\pm$30 Ns horizontal pushes on the trunk, and 90% of 8 Ns backward and 4 Ns forward impulses on the swing foot throughout the gait cycle. Furthermore, the VNMC is resilient to modeling errors and sensor noise much larger than the equivalent uncertainties in the real robot. The results suggest VNMC as a potential alternative to generate robust locomotion in bipedal robots.**

I. INTRODUCTION

State of art locomotion controllers enable bipedal robots to walk outside the laboratory environment [1]–[4]. A typical controller takes high-level goals from a footstep planner, uses a simple dynamics model to plan the corresponding center of mass (COM) trajectories, and generates target joint torques of the full robot that realize these trajectories [5]. Recent implementations of this approach replan the footsteps online to react to unexpected disturbances [1], or account for the full dynamics of the robot to calculate desired joint torques [3], [6]. Other controllers employ more heuristic policies to overcome unexpected disturbances. For example, intuition-based policies that adjust the step length, leg thrust, and trunk lean have demonstrated stable locomotion [2], [7]. Despite these advances, walking controllers have not yet reached the robustness of human control in locomotion, which makes it difficult to use bipedal robots in scenarios such as rescuing lives from natural and man-made disasters.

An alternative control strategy is to imitate the human control of locomotion. Although the human control is not fully understood, various neuromuscular models have been proposed to explain fundamental control mechanisms of human locomotion [8]–[12]. For instance, it has been demonstrated in physics simulations that neural controllers, consisting of central pattern generators and muscle reflex modules, can generate stable 3-D walking [9], [12]. Corresponding bioinspired controllers have been developed to generate walking in humanoid robots [13]–[16]. They demonstrate stable walking with tolerance to moderate disturbances and are often used for miniature humanoid robots [15], [16]. However, the existing bioinspired walking controllers do not demonstrate locomotion that is more robust than the aforementioned robotic controllers.

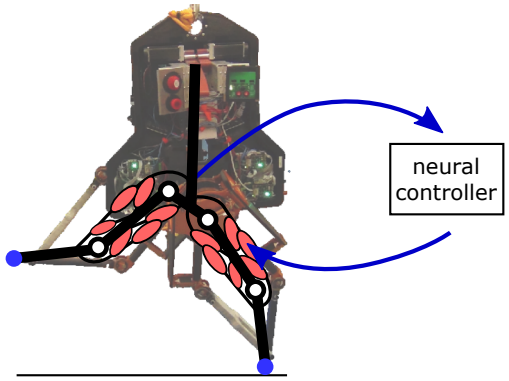

Fig. 1. Virtual neuromuscular control for bipedal robot locomotion. An emulated neuromuscular model is mapped to a robot topology (ATRIAS pictured) to generate desired motor torques.

Here, we seek to control a bipedal robot ATRIAS with a specific neuromuscular human walking model we previously proposed [12] (Fig. 1). This model can generate robust 3-D locomotion on rough terrain (unexpected ground-height changes of $\pm$10 cm), resist external pushes (8 – 86 Ns), and generate diverse locomotion behaviors in simulation. However, it is unclear whether the robust locomotion observed in the simulation transfers to the physical robot, since the dynamics of ATRIAS are significantly different from human dynamics, and sensor noise and actuator saturation may limit performance.

This paper reports on preliminary work of adapting the neuromuscular model as a controller for ATRIAS in simulation. The simulation platform models the existing experimental testbed of ATRIAS constrained to the sagittal plane by a boom (Sec. II). We develop a virtual neuromuscular controller, VNMC, that emulates the neuromuscular model and maps the model to the ATRIAS geometry to generate desired motor torques (Sec. III-A). We optimize the control parameters for maximum ground-height changes (Sec. III-B), which results in ATRIAS walking on a terrain with $\pm$7 cm height changes. We analyze this walking behavior

This work is supported in part by the DARPA M3 program (W91CRB-11-1-0002).

Z. Batts, S. Song, and H. Geyer are with the Robotics Institute, Carnegie Mellon University, 5000 Forbes Avenue, Pittsburgh, PA 15213, USA. {zbatts,smsong,hgeyer}@cmu.edu

TABLE I

SEGMENT PROPERTIES OF ATRIAS AND A HUMAN MODEL [12]

	trunk		upper leg		lower leg		foot		
	COM to hip	mass	length	mass	length	mass	length	height	mass
ATRIAS	10	57.9	50	1.1	50	1.0	-	-	-
human model	35	53.5	46	8.5	46	3.5	20	8	1.25

(unit: cm, kg)

and the robustness of the controller to external and internal disturbances (Sec. IV). The optimized VNMC tolerates 90% of the terrains with ground-height changes up to ± 2 cm. It endures 95% of ± 30 Ns horizontal pushes on the trunk, and 90% of 8 Ns backward and 4 Ns forward impulses on the swing foot through out the gait cycle. In addition, the VNMC is resilient to modeling errors and sensor noise much larger than the corresponding uncertainties in the real robot. The results suggest that the VNMC is a potential alternative to generate robust locomotion in bipedal robots. We discuss the limitations of the current implementation of VNMC and potential outcomes of our work (Sec. V).

II. ATRIAS SIMULATION PLATFORM

ATRIAS is a human-size (1-m leg length and 63-kg body weight) bipedal robot that is designed to concentrate the mass at the trunk [17], which results in segment dynamics different than those of humans (Table I). Each of ATRIAS' legs is a lightweight four-bar linkage that makes point contact with the ground. Two series elastic actuators (SEAs) located at each hip joint drive the four-bar linkage in the sagittal plan. A third gear-motor controls the leg in the frontal plane, which can be used for 3-D locomotion.

In this study, we use a high-fidelity simulation of the ATRIAS platform constrained in the sagittal plane, which was developed and tested in a previous study [18] (Fig. 2, Matlab Simulink/SimMechanics R2014b). The ATRIAS model has 10 internal degrees of freedom (4 for the four-bar linkages, 4 for the SEAs, and 2 for the frontal plane motors). In addition, a boom constrains ATRIAS to a circular track, while the trunk is allowed to pitch. The frontal plane motors are regulated to keep both legs in the sagittal plane. Furthermore, the simulation includes the detailed SEA dynamics and control (max torque: 350 Nm), and dynamic ground contact models that capture stick-slip friction. While we simulate the continuous dynamics of the physical system with a variable time-step solver (ode45, relative error tolerance: 1e-3, absolute error tolerance 1e-4), the control loop runs discretely at 1 kHz to match the control frequency of the actual robot. The simulation includes the encoders used to estimate the position and orientation of the trunk, internal joint angles, and SEA motor torques.

III. VIRTUAL NEUROMUSCULAR CONTROL

A. Virtual Neuromuscular Controller

The virtual neuromuscular controller (VNMC) simulates a neuromuscular model to derive desired joint torques of the ATRIAS robot for walking (Fig. 3). The robot's

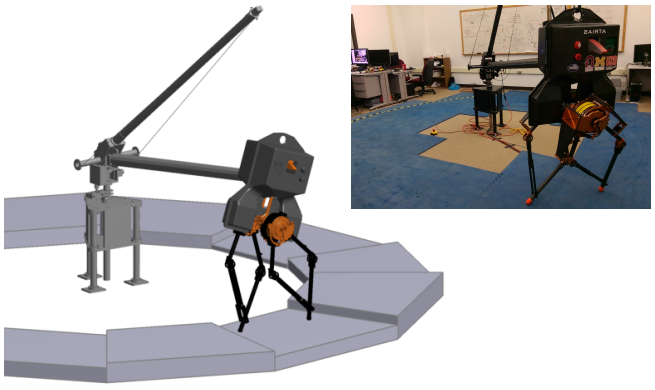

Fig. 2. Simulation of the 2-D experimental testbed of ATRIAS. The top right picture shows the actual testbed of ATRIAS constrained to a circular track by a boom. We use a high-fidelity simulation of this testbed to investigate virtual neuromuscular control.

trunk lean, forward velocity, joint angles and joint torques $(\theta_r, \mathrm{v}_r, \boldsymbol{\varphi}_r, \boldsymbol{\tau}_r)$ are mapped to virtual measurements required to simulate the neuromuscular model, which are the trunk lean, forward velocity, joint angles, loading force on the legs, and the foot-contact information $(\theta_v, \mathrm{v}_v, \boldsymbol{\varphi}_v, \mathbf{f}_v, \mathbf{c}_v)$. The neuromuscular model outputs virtual joint torques $(\boldsymbol{\tau}_v)$ that are mapped to desired robot joint torques $(\hat{\boldsymbol{\tau}}_r)$, which are then tracked by the SEA controller.

The neuromuscular model of the VNMC is adapted from the sagittal hip and knee components of the human control model in [12]. The model includes a skeletal system, muscle-tendon units, and a neural circuitry. The skeletal system is a kinematic chain that comprises the trunk, thigh and shank segments connected by the hip and knee joints. The skeletal system is synchronized with ATRIAS, in that the trunks, hips and the feet are collocated. Monoarticular and biarticular muscles generate virtual torques around the hip and knee joints. The neural circuits control the virtual muscles by generating muscle stimulations based on the neural sensory data from the musculoskeletal system. We treat the neuromuscular model as a black box that generates virtual joint torques based on the virtual measurements, $\boldsymbol{\tau}_v = \boldsymbol{\tau}_v(\theta_v, \mathrm{v}_v, \boldsymbol{\varphi}_v, \mathbf{f}_v, \mathbf{c}_v)$. (See [12] for details on the control circuitry.)

The remaining part of the VNMC converts the sensory data of the robot to the virtual measurements, Φ_φ: $(\theta_r, \mathrm{v}_r, \boldsymbol{\varphi}_r, \boldsymbol{\tau}_r) \rightarrow (\theta_v, \mathrm{v}_v, \boldsymbol{\varphi}_v, \mathbf{f}_v, \mathbf{c}_v)$, and the virtual torques to desired robot joint torques, Φ_τ: $\boldsymbol{\tau}_v \rightarrow \hat{\boldsymbol{\tau}}_r$. The trunk lean and the forward velocity of the virtual skeleton are identical to that of ATRIAS, $\{\theta_v, v_v\} = \{\theta_r, v_r\}$. The remaining measurements are converted through geometric transformations. The joint angles of the skeletal system, $\boldsymbol{\varphi}_v = \left(\varphi_v^{R1}, \varphi_v^{R2}, \varphi_v^{L1}, \varphi_v^{L2}\right)$, are mapped from the joint angles of the robot, $\boldsymbol{\varphi}_r = \left(\varphi_r^{R1}, \varphi_r^{R2}, \varphi_r^{L1}, \varphi_r^{L2}\right)$. For instance, the kinematic relation for the joints of the right (R) leg is

$$\varphi_v^{R1} = \frac{1}{2}\left(-\pi + \varphi_r^{R1} + \varphi_r^{R2} + \varphi_v^{R2}\right) \tag{1}$$

$$\varphi_v^{R2} = 2\sin^{-1}\left(\frac{l_r}{l_v}\cos\left(\frac{\varphi_r^{R2} - \varphi_r^{R1}}{2}\right)\right) \tag{2}$$

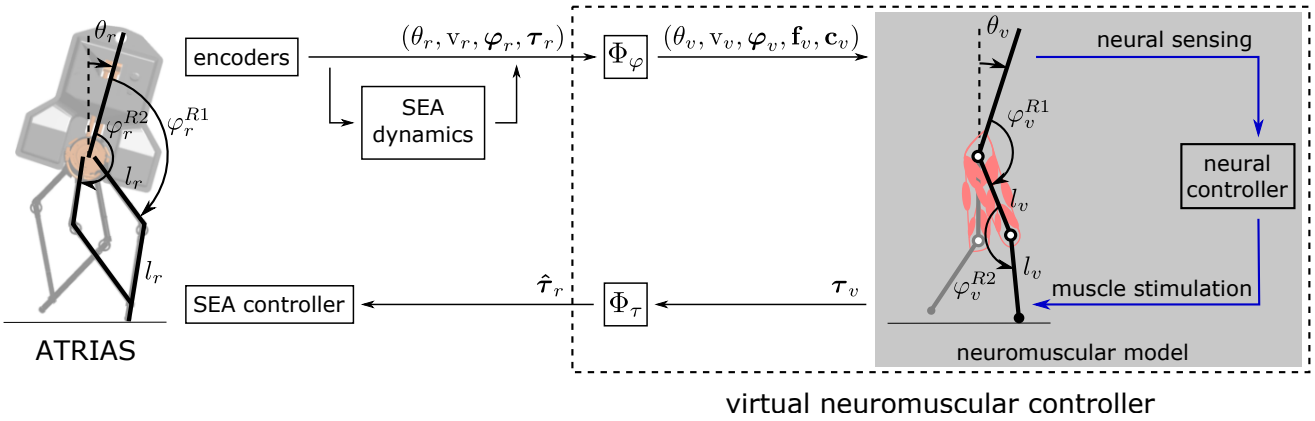

Fig. 3. Virtual neuromuscular controller on ATRIAS. The encoders on the ATRIAS model measure the states of the robot used by the VNMC. The SEA controller tracks desired torques to drive the ATRIAS model. The desired torques are generated by VNMC, which simulates a neuromuscular model that is mapped to the robot geometry.

where l_r and l_v are the segment lengths (the thigh and shank are equal in length) of the robot and virtual legs, respectively. We model mechanical limits of ATRIAS that prevent the right hand side of Eq. (2) from reaching singularity. (All the mappings are the same for the left leg.) The loads on the legs, $\mathbf{f}_v = \left(\mathrm{f}_v^R, \mathrm{f}_v^L\right)$, are the components of the ground reaction forces that act in the direction from the feet to the hips. These are estimated, assuming quasi-static equilibrium, from the robot joint torques, $\boldsymbol{\tau}_r = \left(\tau_r^{R1}, \tau_r^{R2}, \tau_r^{L1}, \tau_r^{L2}\right)$, as

$$\mathrm{f}_v^R = \frac{\tau_r^{R1} - \tau_r^{R2}}{2\, l_r \sin\left(\frac{\varphi_r^{R2} - \varphi_r^{R1}}{2}\right)}. \tag{3}$$

The boolean vector, $\mathbf{c}_v = \left(\mathrm{c}_v^R, \mathrm{c}_v^L\right)$, indicates whether the legs are in contact with the ground. We assume a contact is made if the leg force (f_v^R or f_v^L) exceeds 25% of body-weight. Finally, the virtual joint torques, $\boldsymbol{\tau}_v = \left(\tau_v^{R1}, \tau_v^{R2}, \tau_v^{L1}, \tau_v^{L2}\right)$, are mapped to desired robot actuator torques, $\hat{\boldsymbol{\tau}}_r = \left(\hat{\tau}_r^{R1}, \hat{\tau}_r^{R2}, \hat{\tau}_r^{L1}, \hat{\tau}_r^{L2}\right)$, as

$$[\hat{\tau}_r^{R1}, \hat{\tau}_r^{R2}]^T = \Phi_\tau^T [\tau_v^{R1}, \tau_v^{R2}]^T \tag{4}$$

using the Jacobian

$$\Phi_\tau = \begin{bmatrix} \frac{1+k}{2} & \frac{1-k}{2} \\ k & -k \end{bmatrix} \tag{5}$$

between virtual and robot joint velocities with

$$k = \frac{l_r \sin\left(\frac{\varphi_r^{R2} - \varphi_r^{R1}}{2}\right)}{l_v \cos\left(\frac{\varphi_v^{R2}}{2}\right)}. \tag{6}$$

The virtual knee angles (φ_v^{R2} and φ_v^{L2}) are saturated at 179 deg to avoid singularity in Eq. (6), and the desired torques ($\hat{\boldsymbol{\tau}}_r$) are saturated at the maximum actuator torques, ± 350 Nm.

B. Optimization of the VNMC parameters

We optimize the control parameters, $\mathbf{p} \in \mathbb{R}^n$ ($n = 50$), of the black box neuromuscular model to generate robust walking. Specifically, we simulate ATRIAS walking on a circular track with one-meter-long flat ground tiles of randomly varying heights and use optimization to find the largest height difference $|\Delta \mathrm{h}_{max}|$ that ATRIAS successfully traverses. For that purpose, we construct the cost function as

$$J(\mathbf{p}, |\Delta \mathrm{h}_{max}|) = \begin{cases} \mathrm{d}_{tgt} - \mathrm{d}_{walk}, & \text{if } \mathrm{d}_{walk} < \mathrm{d}_{tgt} \\ -|\Delta \mathrm{h}_{max}|, & \text{otherwise} \end{cases}, \tag{7}$$

where d_{tgt} is a target travel distance ($\mathrm{d}_{tgt} = 30$ m ≈ 2.5 laps), and d_{walk} is the distance the model walks before falling. The cost function was designed considering two possible simulation outcomes: falling and completing the course. First, if the model fails to reach the target distance ($\mathrm{d}_{walk} < \mathrm{d}_{tgt}$), the cost decreases the further the model walks. Second, if the model successfully traverses the track ($d_{walk} \geq d_{tgt}$), the cost decreases as the largest ground-height change ($|\Delta \mathrm{h}_{max}|$) increases, which is also an optimization parameter. The initial seed parameters for optimization were hand-tuned on flat terrain (not presented in this paper). We use the covariance matrix adaptation evolution strategy [19] to optimize the control parameters for minimum cost.

IV. RESULTS

A. Optimized Walking for Rough Terrain

With the optimized VNMC, ATRIAS can walk on a terrain with maximum height differences of ± 7 cm (see accompanying video). Figure 4 shows kinematic and kinetic data for 13 seconds of this walking behavior, during which the robot traverses the maximum height changes. The robot gains and loses forward velocity (v_r) as it descends and ascends the tiles, respectively. The trunk lean (θ_r) and step length, which are recognized as important factors in controlling walking speed [20], [21], show a close trend with the forward velocity. During the first few steps, vertical ground reaction forces (GRFs) show the characteristic double-hump pattern of human walking. In the later steps, the GRFs show chatter, which seems to emerge from the vibration of the swing leg. If the swing leg oscillates, the stance control attempts to

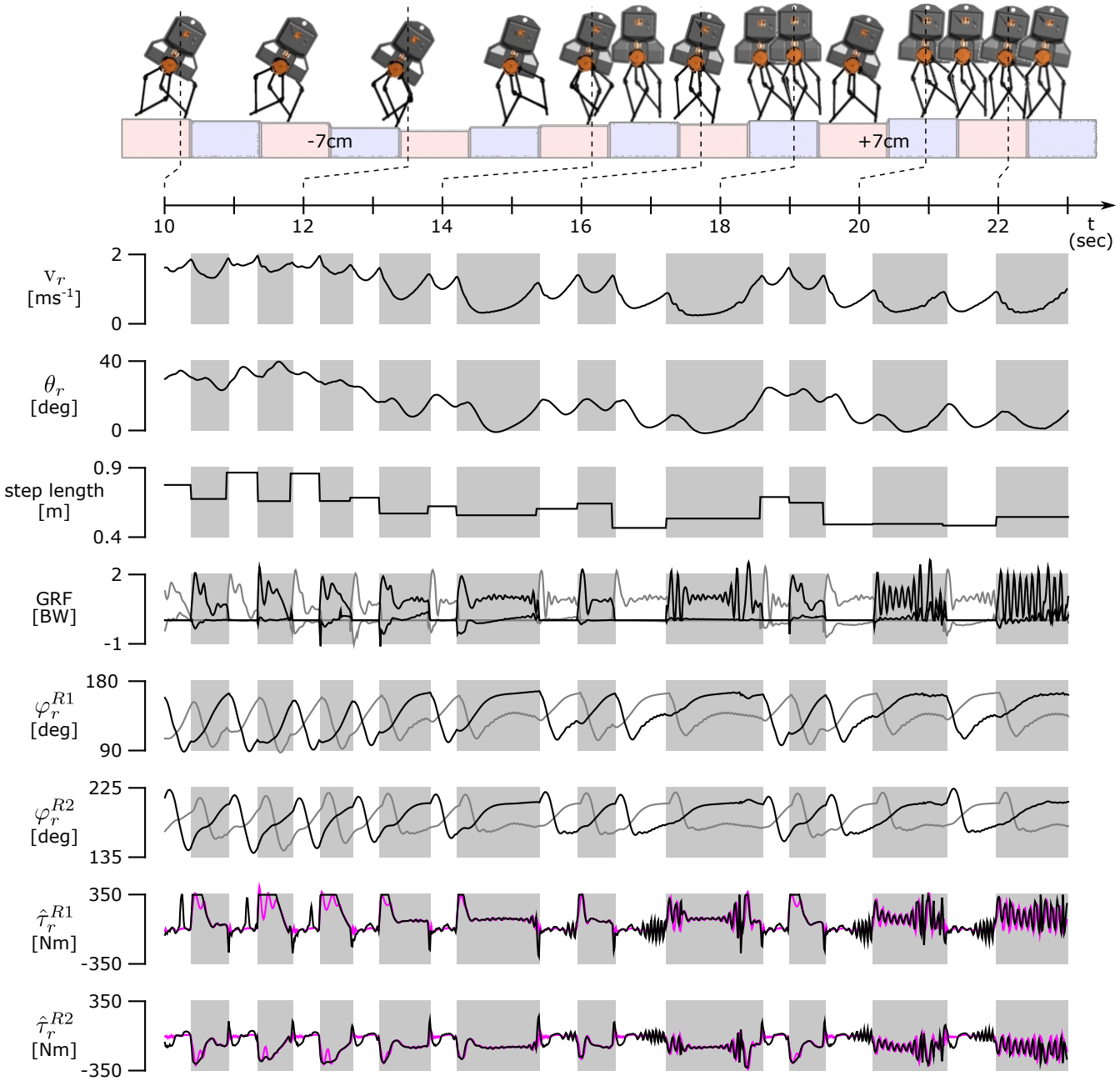

Fig. 4. Kinematic and kinetic data while walking on rough terrain. The top panel shows snapshots projected to a 2-D plane of ATRIAS every 1 second walking on a $\pm$ 7cm terrain. The panels below show the forward velocity v_r, trunk lean θ_r, step length, right leg ground reaction forces (gray: left leg; scaled to body weight (BW)), right leg joint angles φ_r^{R1} and φ_r^{R2} (gray: left leg), and right leg desired joint torques $\hat{\tau}_r^{R1}$ and $\hat{\tau}_r^{R2}$ (magenta: SEA torques). Stance phases of the right leg are marked by gray background.

compensate it by producing similar oscillating torques that propagate to the GRFs. Since this undesired behavior is not observed in the original human neuromuscular model, it may originate in the SEA dynamics and the discretized controller. Nevertheless, VNMC adapts to the unobserved terrain by modulating the forward velocity, step lengths, gait periods, and joint trajectories.

B. Robustness Test of the Optimized VNMC

We evaluate the robustness of the optimized VNMC by simulating a variety of disturbances that are typical in a real-world environment, including ground-height disturbances and external pushes. In addition, we examine the controller tolerance to modeling error and sensor noise.

We assess the robustness of the controller against ground-height disturbances by evaluating the success rate of traversing sets of random terrains with different levels of difficulty. We test on 10 sets of terrains with varying ground-height. Each set consists of 100 random 30-meter-long terrains with a common maximum ground-height change ($|\Delta h_{max}|$) that ranges from $\pm$1 cm to $\pm$10 cm across the sets. We count the

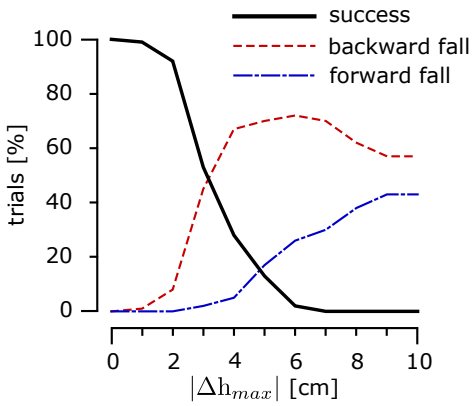

Fig. 5. Robustness to rough terrain. Shown are the percentage of success (black line), backward fall (red dashed line), and forward fall (blue dashed line) in walking trials over sets of terrains with maximum ground-height differences $|\Delta h_{max}|$ of ± 1 cm to ± 10 cm.

trials for which ATRIAS successfully traverses the terrains of each set (Fig. 5). The success rate is over 90% up to ± 2 cm terrains, significantly decreases to 50% at ± 3 cm, and is zero for all the terrains over ± 7 cm. Up to ± 7 cm terrains, the robot tends to fall backward often losing forward momentum while walking up the terrains. We speculate that the absence of the ankle joint, which provides large forward propulsion in the original human model [21], limits the robustness against ground disturbances. In addition, the original neuromuscular model modulates the trunk lean to generate additional propulsion [21]; however, the COM of ATRIAS' trunk is close to the hip, which attenuates the effect of this strategy. For terrains with larger height changes ($|\Delta h_{max}| \geq 8$ cm), the proportion of falling forward increases. This is because ATRIAS more often kicks the vertical face of the tiles, which causes the robot to trip forward.

In addition to studying rough ground locomotion, we test the controller against external pushes to the trunk and the swing foot while walking on flat ground. First, we apply constant horizontal forces ranging from $[-1000, 1000]$ N for 100 ms on the COM of the trunk at different phases of the gait cycle. We test for 20 different strides and evaluate the success rate (Fig. 6-A). The controller endures about 95% of ± 30 Ns pushes throughout the gait cycle. In general, it can withstand larger backward pushes than forward pushes. It can also tolerate larger pushes around heel strike, which is when the kinetic energy of the robot is maximal during the gait cycle (refer to v_r data in Fig. 4). Second, we conduct a similar experiment on the swing foot with forces ranging from $[-600, 600]$ N (Fig. 6-B). The robot can resist about 90% of the impulses of -8 Ns and $+4$ Ns. The controller is more robust to forward impulses during early swing, since the swing foot accelerates forward at this phase in normal walking. To backward impulses, it is most robust during mid-swing when the forward velocity of the foot is maximal. The left leg is more sensitive than the right leg to backward pushes during late swing. This asymmetry is likely due to the circular track, which already forces the left leg (the inner

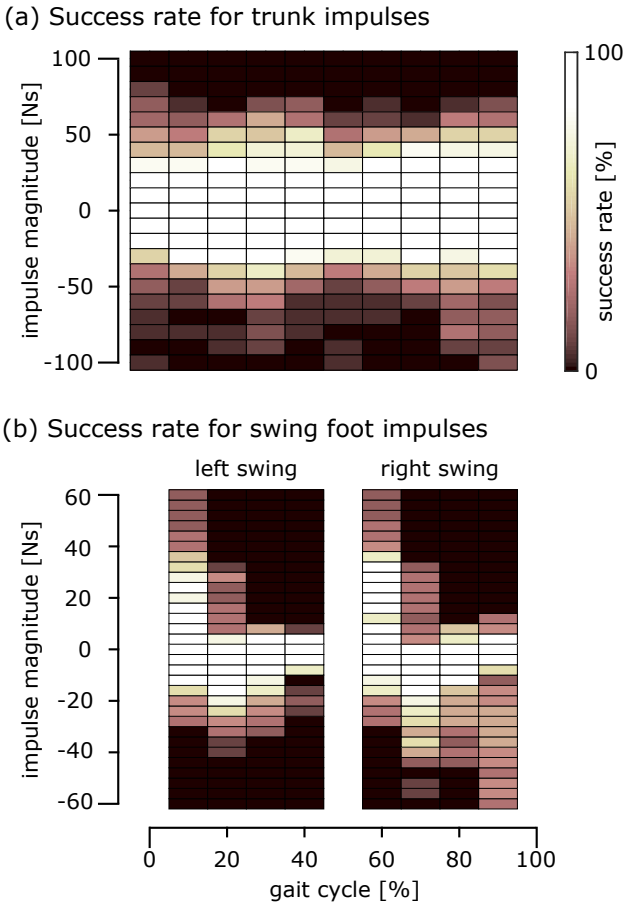

Fig. 6. Robustness to external pushes. (a) Success rate for horizontal impulses to the trunk COM for the range of $[-100, 100]$ Ns with 10 Ns resolution for every 10% of the gait cycle. (b) Success rate for horizontal impulses to the swing foot in the range of $[-60, 60]$ Ns with 4 Ns resolution.

leg) to swing less than the right in nominal walking.

We also evaluate the resilience of the optimized VNMC against internal disturbances: modeling errors and sensor noise (Table II). For modeling errors, we find the range of trunk and leg inertias and the SEA spring properties for which the robot can maintain walking. In general, VNMC is resilient to modeling errors. For example, it can withstand three times increased leg inertia and five times stiffer SEA springs. Based on a previous study with the simulation and hardware of ATRIAS [18], the uncertainties in the actual dynamic properties are much less than the modeling errors VNMC tolerates. Similarly, we add Gaussian noise to the encoder signals until the robot falls down, and VNMC withstands sensor noise much larger than that expected in the actual robot. The robot walks with up to $\sigma = 0.1$ deg of noise in all ten encoders that measure internal DOFs, which is much larger ($\times$1e6) than the error of the 32-bit encoders on the robot. The VNMC is insensitive to the global frame measurements used in the control, which are the trunk lean (θ_r) and forward velocity (v_r) (Table II). This indicates that the controller does not require high-fidelity accelerometers and gyroscopes to measure this data. On the other hand, it implies that the optimized VNMC does not

TABLE II

SENSITIVITY TO MODELING ERRORS AND SENSOR NOISE. DYNAMIC PROPERTIES ARE THE MASS AND INERTIA OF THE TRUNK AND LEGS, AND THE ELASTICITY AND DAMPING OF THE SEA SPRINGS.

dynamic properties	min ... max	noise	max σ
trunk	80% ... 140%	φ_r	0.1 deg
leg	30% ... 330%	θ_r	27.5 deg
SEA spring	80% ... 560%	v_r	102 ms^{-1}

fully use the functionalities of the original neuromuscular control, which stabilizes the trunk and modulates the foot placement based on these measurements. Perhaps the VNMC would be more robust by taking full advantage of these control functionalities.

V. SUMMARY AND FUTURE DIRECTION

In this paper, we proposed a virtual neuromuscular controller, VNMC, to generate robust walking for the bipedal robot ATRIAS. VNMC simulates a human neuromuscular model, and maps the model to ATRIAS to generate desired joint torques. We optimized the control parameters to tolerate maximum ground-height changes, which resulted in ATRIAS walking on a ± 7 cm terrain. We tested the resulting controller against external and internal disturbances. Using the controller, ATRIAS tolerates about 90% of the terrains with ground-height changes of ± 2 cm. It endures 95% of ± 30 Ns horizontal pushes on the trunk, and 90% of 8 Ns backward and 4 Ns forward impulses on the swing foot throughout the gait cycle. In addition, VNMC is resilient to modeling errors and sensor noise much larger than the equivalent uncertainties in the real robot. The results suggest VNMC as a potential alternative to generate robust locomotion in bipedal robots.

The current VNMC is less robust than the original neuromuscular human model, which tolerates over ± 20 cm in 2-D [22]. We speculate that three main reasons account for this reduction in performance. First, the segment properties of the robot are different from that of humans. For example, ATRIAS does not have feet which generate large propulsion in the human model (Sec. IV-B). Second, the SEA dynamics and the discretized control loop seem to cause undesired high frequency oscillations in the walking motion (Sec. IV-A). Third, the VNMC does not seem to use the full functionality of the original neuromuscular control model (Sec. IV-B).

We plan to address the latter two problems in future work, and transfer the VNMC to the ATRIAS experimental setup. Our immediate goal is to demonstrate and evaluate the control in the 2-D testbed. Eventually, we aim to extend VNMC to generate 3-D locomotion in bipedal robots.

REFERENCES

[1] J. Urata, K. Nishiwaki, Y. Nakanishi, K. Okada, S. Kagami, and M. Inaba, "Online decision of foot placement using singular lq preview regulation," in *Humanoid Robots (Humanoids), 2011 11th IEEE-RAS International Conference on*. IEEE, 2011, pp. 13–18.

[2] G. Nelson, A. Saunders, N. Neville, B. Swilling, J. Bondaryk, D. Billings, C. Lee, R. Playter, and M. Raibert, "Petman: A humanoid robot for testing chemical protective clothing," *ł*, vol. 30, no. 4, pp. 372–377, 2012.

[3] S. Feng, E. Whitman, X. Xinjilefu, and C. G. Atkeson, "Optimization based full body control for the atlas robot," in *Humanoid Robots (Humanoids), 2014 14th IEEE-RAS International Conference on*. IEEE, 2014.

[4] M. Johnson, B. Shrewsbury, S. Bertrand, T. Wu, D. Duran, M. Floyd, P. Abeles, D. Stephen, N. Mertins, A. Lesman *et al.*, "Team ihmc's lessons learned from the darpa robotics challenge trials," *Journal of Field Robotics*, vol. 32, no. 2, pp. 192–208, 2015.

[5] S. Kajita, F. Kanehiro, K. Kaneko, K. Fujiwara, K. Harada, K. Yokoi, and H. Hirukawa, "Biped walking pattern generation by using preview control of zero-moment point," in *Robotics and Automation, 2003. Proceedings. ICRA'03. IEEE International Conference on*, vol. 2. IEEE, 2003, pp. 1620–1626.

[6] S. Kuindersma, F. Permenter, and R. Tedrake, "An efficiently solvable quadratic program for stabilizing dynamic locomotion," in *Robotics and Automation (ICRA), 2014 IEEE International Conference on*. IEEE, 2014, pp. 2589–2594.

[7] M. H. Raibert *et al.*, *Legged robots that balance*. MIT press Cambridge, MA, 1986, vol. 3.

[8] G. Taga, "A model of the neuro-musculo-skeletal system for human locomotion," *Biological cybernetics*, vol. 73, no. 2, pp. 97–111, 1995.

[9] K. Hase and N. Yamazaki, "Computer simulation study of human locomotion with a three-dimensional entire-body neuro-musculo-skeletal model. i. acquisition of normal walking." *JSME International Journal Series C*, vol. 45, no. 4, pp. 1040–1050, 2002.

[10] M. Günther and H. Ruder, "Synthesis of two-dimensional human walking: a test of the λ-model," *Biological cybernetics*, vol. 89, no. 2, pp. 89–106, 2003.

[11] H. Geyer and H. Herr, "A muscle-reflex model that encodes principles of legged mechanics produces human walking dynamics and muscle activities," *Neural Systems and Rehabilitation Engineering, IEEE Transactions on*, vol. 18, no. 3, pp. 263–273, 2010.

[12] S. Song and H. Geyer, "A neural circuitry that emphasizes spinal feedback generates diverse behaviours of human locomotion," *The Journal of physiology*, 2015.

[13] R. Héliot and B. Espiau, "Multisensor input for cpg-based sensory—motor coordination," *Robotics, IEEE Transactions on*, vol. 24, no. 1, pp. 191–195, 2008.

[14] J. Morimoto, G. Endo, J. Nakanishi, and G. Cheng, "A biologically inspired biped locomotion strategy for humanoid robots: Modulation of sinusoidal patterns by a coupled oscillator model," *Robotics, IEEE Transactions on*, vol. 24, no. 1, pp. 185–191, 2008.

[15] R. Zaier and S. Kanda, "Adaptive locomotion controller and reflex system for humanoid robots," in *Intelligent Robots and Systems, 2008. IROS 2008. IEEE/RSJ International Conference on*. IEEE, 2008, pp. 2492–2497.

[16] J. Nassour, P. Hénaff, F. Benouezdou, and G. Cheng, "Multi-layered multi-pattern cpg for adaptive locomotion of humanoid robots," *Biological cybernetics*, vol. 108, no. 3, pp. 291–303, 2014.

[17] A. Ramezani, J. W. Hurst, K. A. Hamed, and J. Grizzle, "Performance analysis and feedback control of atrias, a three-dimensional bipedal robot," *Journal of Dynamic Systems, Measurement, and Control*, vol. 136, no. 2, p. 021012, 2014.

[18] W. C. Martin, A. Wu, and H. Geyer, "Robust spring mass model running for a physical bipedal robot," in *Robotics and Automation (ICRA), 2015 IEEE International Conference on*. IEEE, 2015.

[19] N. Hansen, "The cma evolution strategy: A comparing review," *Towards a New Evolutionary Computation. Advances on Estimation of Distribution Algorithms. Springer*, p. 75.102, 2006.

[20] D. G. Hobbelen and M. Wisse, "Controlling the walking speed in limit cycle walking," *The International Journal of Robotics Research*, vol. 27, no. 9, pp. 989–1005, 2008.

[21] S. Song and H. Geyer, "Regulating speed and generating large speed transitions in a neuromuscular human walking model," in *Robotics and Automation (ICRA), 2012 IEEE International Conference on*. IEEE, 2012, pp. 511–516.

[22] S. Song, R. Desai, and H. Geyer, "Integration of an adaptive swing control into a neuromuscular human walking model," in *Engineering in Medicine and Biology Society (EMBC), 2013 35th Annual International Conference of the IEEE*. IEEE, 2013, pp. 4915–4918.